Exploring the applicability of the Q-G omega equation to meteorological case studies using IDV

Author: Paula Caballero Roca.
*Facultat de Física, Universitat de Barcelona, Diagonal 645, 08028 Barcelona, Spain.**

Advisor: Dr. Ileana Bladé Mendoza

Abstract: In the framework of quasi-geostrophic theory different formulations of the omega equation for the diagnosis of vertical motion in synoptic-scale weather systems have been proposed. Here we will focus on the traditional and the $\vec{Q}$-vector adiabatic forms of this equation and compute them using the Jython programming environment of the IDV software to assess their applicability to the qualitative analysis of vertical motion in various case studies. We will also attempt to compute the diabatic contribution to evaluate to what extent it is reasonable to neglect it when performing this quasi-geostrophic diagnostic.

I. INTRODUCTION

Dynamic meteorology is primarily concerned with interpreting the observed structure of large-scale atmospheric motions using the equations for the conservation of momentum, mass and energy. Although these equations are rather complex, the fact that the flow for extratropical synoptic-scale weather systems is approximately in geostrophic and hydrostatic balance allows for a simplified form of these equations, the quasi-geostrophic system, which constitutes the basis of quasi-geostrophic theory (Q-G theory). Q-G theory emerged in the decade of the fifties and has established itself as the cornerstone of modern dynamic meteorology since it allows one to describe the baroclinic behavior of large-scale atmospheric motions qualitatively and quantitatively.

The combination of the Q-G vorticity and thermodynamic energy equations gives rise to the Q-G omega equation, which provides a diagnostic for vertical motions in the atmosphere [1]. Its conventional adiabatic form can be written as

$$\sigma\left(\nabla^2+\frac{f_0^2}{\sigma}\frac{\partial^2}{\partial p^2}\right)\omega = f_0\frac{\partial}{\partial p}\left[\vec{V}_g\cdot\nabla\left(\frac{1}{f_0}\nabla^2\phi+f\right)\right] + \nabla^2\left[\vec{V}_g\cdot\left(-\frac{\partial\phi}{\partial p}\right)\right], \quad (1)$$

where $\omega \propto -w$ is the vertical pressure velocity, being w the vertical velocity; $\sigma = -(RT/p)(\partial \ln\theta/\partial p)$ is the stability parameter, being θ the potential temperature; $f_0 = 2\Omega\sin(\varphi)$ is the Coriolis parameter; $\vec{V}_g$ is the geostrophic wind; $\frac{1}{f_0}\nabla^2\phi$ and f are the geostrophic relative vorticity and the planetary vorticity, respectively; and p, ϕ represent the pressure and the geopotential, respectively.

The power of this expression lies in the fact that it provides an estimate of ω independent of accurate observations of the wind. The first term in the RHS is linked to the vertical derivative of the absolute vorticity advection by the geostrophic wind (AVA). Given the hydrostatic equation, the second term is proportional to minus the Laplacian of temperature advection (LTA), which, for wave-like perturbations is qualitatively similar to the temperature advection (TA) itself. Additionally, if one assumes that the vertical motion field exhibits a sinusoidal vertical profile, the LHS term is, to first order, proportional to $-\omega$ or w. More accurately, the fact that the LHS operator contains vertical derivatives implies that the response to a forcing given by the RHS will not be localized but will be vertically spread above and below the level in which it occurs, particularly for large-scale disturbances. Hence qualitatively, we have $\mathrm{w} \simeq \mathrm{DVA} + \mathrm{TA}$, where DVA stands for differential vorticity advection. From these considerations, it is deduced that regions that are characterized by cyclonic (anticyclonic) absolute vorticity advection increasing with height will exhibit upward (downward) vertical motion and those displaying a local maximum in warm (cold) temperature advection will be related to ascent (descent).

Even though the two RHS terms of Eq. (1) appear to have separate physical interpretations, in practice there often exists a considerable amount of cancellation between them, yielding a non-conclusive result for the sign of the vertical motion. To overcome this issue, Trenberth [2] suggested an alternative approach to understanding the forcing of quasi-geostrophic vertical motions in the atmosphere in which the RHS of Eq. (1) can be approximated in terms of the advection of geostrophic absolute vorticity by the thermal wind. This method allows assessment of the vertical motion directly from the geopotential height and thickness contours. Although this approach eliminates the cancellation problem, it entails an approximation compared to the Eq. (1), which may restrict its applicability: the neglect of the so-called deformation term, which is related to the stretching and shearing deformations in the atmosphere. Trenberth, however, argued that the deformation term was only relevant in frontal regions. Martin [3] went further in examining its importance by studying its role during the evolution of a typical mid-latitude cyclone. He

* Electronic address: pcabalro39@alumnes.ub.edu

concluded that the deformation forcing is negligible during the development and early mature stages of a cyclone life cycle, but it cannot be omitted as the cyclone begins to occlude and late in its life cycle. Parallelly to Trenberth, Hoskins et al. [4] presented yet another form of the traditional omega equation (1) that also constitutes an effective means of dealing with the Q-G cancellation problem and does not neglect the deformation term. The traditional form of the Q-G omega equation also includes the deformation term, but the $\vec{Q}$-vector formulation of Hoskins has the additional advantage that it does not involve calculations of vertical derivatives, apart from those inherent to the derivation of the temperature field from the hydrostatic equation. Its adiabatic expression can be written as [5]

$$\sigma\left(\nabla^2 + \frac{f_0^2}{\sigma}\frac{\partial^2}{\partial p^2}\right)\omega = -2\nabla\cdot\vec{Q}\ , \qquad (2)$$

where the $\vec{Q}$-vector [5] is given by:

$$\vec{Q} \equiv (Q_1, Q_2) = \left(-\frac{R}{p}\frac{\partial\vec{V}_g}{\partial x}\cdot\nabla\mathrm{T}, -\frac{R}{p}\frac{\partial\vec{V}_g}{\partial y}\cdot\nabla\mathrm{T}\right), \qquad (3)$$

where R is the constant for dry air. According to Eq. (2) and (3), convergence (divergence) of the $\vec{\mathrm{Q}}$-vector implies upward (downward) vertical motion.

This project then aims to explore the various methods for diagnosing vertical motion in mid-latitude weather systems in the framework of Q-G theory and assess their applicability to a few case studies. For brevity, we will not explore the Trenberth approach, but we will focus on the traditional and the $\vec{Q}$-vector formulations of the Q-G omega equation.

II. DATA AND METHODOLOGY

We will use the visualization tool IDV (Integrated Data Viewer) from Unidata [6], a freely available software that enables one to visualize and analyze three-dimensional geophysical data. IDV also provides a Jython programming environment that we will use to compute the different terms in the various formulations of the Q-G omega equation.

We will perform the analysis using MERRA-2 data [7] (Modern-Era Retrospective analysis for Research and Applications, version 2), which is a database of meteorological variables generated by the Global Modeling and Assimilation Office from the Goddard Space Flight Center (NASA). It is based on reanalysis data and covers the period from 1980 to the present, being regularly updated.

Reanalysis data are corrected and improved forecasts, built-up by assimilating data acquired from meteorological ground stations and satellites into a numerical model in order to make the predictions dynamically adjusted to the observations. The power of these data sources is that they are often publicly available and provide the best three-dimensional description of past weather, being globally complete and consistent in time.

Using IDV, the DVA term in Eq. (1) has been computed by approximating the vertical derivatives by centered finite differences. The minus Laplacian of thermal advection (LTA) term has also been explicitly calculated and added to the DVA to obtain the complete RHS of Eq. (1) and compare it with the also computed RHS of Eq. (2) as well as the analyzed omega. Both RHS have then been divided by the static stability parameter σ using a constant value ($2.5\cdot10^{-6}\ m^2Pa^{-2}s^{-2}$) as is customary [5]. Yet, the units of the fields thus obtained differ from those of the analyzed omega because the LHS operator in these equations cannot be easily inverted. It will thus be meaningless to attempt a quantitative comparison of vertical motion estimates; instead, a qualitative study will be performed, taking into account that one should not anticipate a perfect match between the analyzed omega and the Q-G diagnosis.

All displayed fields are smoothed out with a circular aperture smoothing. Importantly the smoothing also needs to be applied before multiplying fields that are themselves the result of nonlinear multiplications, to avoid aliasing of small-scale noise.

Finally, the examination of the three-dimensional isosurfaces of the vertical pressure velocity has allowed us to infer the level of maximum vertical motion for the various case studies. It has been found that it is around 600-hPa for the textbook case and about 700-hPa for the chosen case studies; hence those have been the levels used for the calculations.

III. A FIRST APPROACH: ANALYZING A TEXTBOOK CASE STUDY

We will begin by analyzing the textbook mid-latitude surface low-pressure system accompanied by an upper-level trough depicted in Fig. 1 [8].

From the geopotential height field at the 600-hPa level, one would expect a local maximum of absolute vorticity advection along the trough axis, yielding cyclonic AVA ahead of the trough and anticyclonic AVA behind it. Likewise, contrasting the sea-level pressure and 600-hPa geopotential height fields, one would anticipate wind veering (backing) and, therefore, warm (cold) TA ahead of (behind) the trough. From these considerations, an area of ascent (descent) would be expected to the east (west) of the trough axis, and indeed this is what one can observe in each estimate of omega shown in Fig. 1. In this case, there is little cancellation between the DVA (Fig. 1A) and the LTA (Fig. 1B), with both terms making approximately equal contributions. When comparing the traditional and the $\vec{Q}$-vector forms of the Q-G omega equation, even though they are mathematically equivalent, one should not expect a perfect agreement since the RHS term of Eq. (1) entails approximating a vertical derivative (the DVA term) while the RHS of Eq. (2) only involves horizontal derivatives. Nevertheless, one can see that there exists a reasonably good agreement between the diagnosis given by the traditional Q-G omega equation, the divergence of the $\vec{Q}$-vector, and the analyzed omega, particularly in the vicinity of the trough.

This textbook case should then be taken as an illustration of how well the various formulations of the Q-G omega equation

apply when the quasi-geostrophic assumptions are satisfied. Note that these assumptions are based on the fulfillment of the hydrostatic and geostrophic balances and include the neglect of friction, horizontal advection of momentum by the ageostrophic wind, vertical advection of momentum, advection of the ageostrophic momentum by the geostrophic wind and orographic forcing.
Next, we will discuss to what extent the usefulness of these diagnostics can be generalized to other case studies.

IV. DEVIATIONS FROM Q-G THEORY: ANALYSIS OF PARTICULAR CASE STUDIES

In the course of this work, we have examined many case studies, but here we will focus on three particular examples chosen to illustrate how one term in RHS of Eq. (1) may contribute more than the other, the ubiquity of the cancellation problem, and the advantages of the $\vec{Q}$-vector formulation compared to the traditional form of the Q-G omega equation.

A. Storm Aurore, 21/10/21 (18:00 UTC) – 700 hPa

The analyzed omega field (Fig. 2E) for this storm does not exhibit a simple structure: there is ascent in northern Scandinavia and the Baltic Sea, together with downward motion in the southern UK, Norway, Netherlands and Poland. A diagnosis based on a separate analysis of the two RHS terms of Eq. (1) would lead to non-conclusive results since both fields are rather noisy despite the smoothing (Fig. 2A and Fig. 2B). Additionally, there is an area of cancellation over the Baltics and Belarus and, according to Fig. 2C, neither term is dominant.
Examining the RHS of the $\vec{Q}$-vector (Fig. 2D) and the traditional (Fig. 2C) formulations of the Q-G omega equation, delivers a similar diagnosis: both indicate ascent from Denmark to Southern Finland and descent from Northern Germany to Lithuania. These displays are less noisy than the DVA and LTA terms and present wider areas of upward and downward vertical motion that fairly agree with the actual one, inferred from the analyzed omega field. Hence, in this case, both the traditional form of the Q-G omega equation and the divergence of the $\vec{Q}$-vector provide a somewhat muddled but acceptable diagnosis for vertical motion.

B. Storm Eunice, 18/02/22 (06:00 UTC) – 700 hPa

The analyzed omega field (Fig. 2K) exhibits a large area of ascent north and northeast of the upper-level trough and a significant region of descent south and to the rear of the trough. This pattern is difficult to glean from just comparing the DVA and LTA terms of Eq. (1) (Fig. 2G and Fig. 2H, respectively) since they present a large amount of cancellation in this region. However, from their sum, shown in Fig. 2I, it can be seen that, in this case, the LTA term dominates.

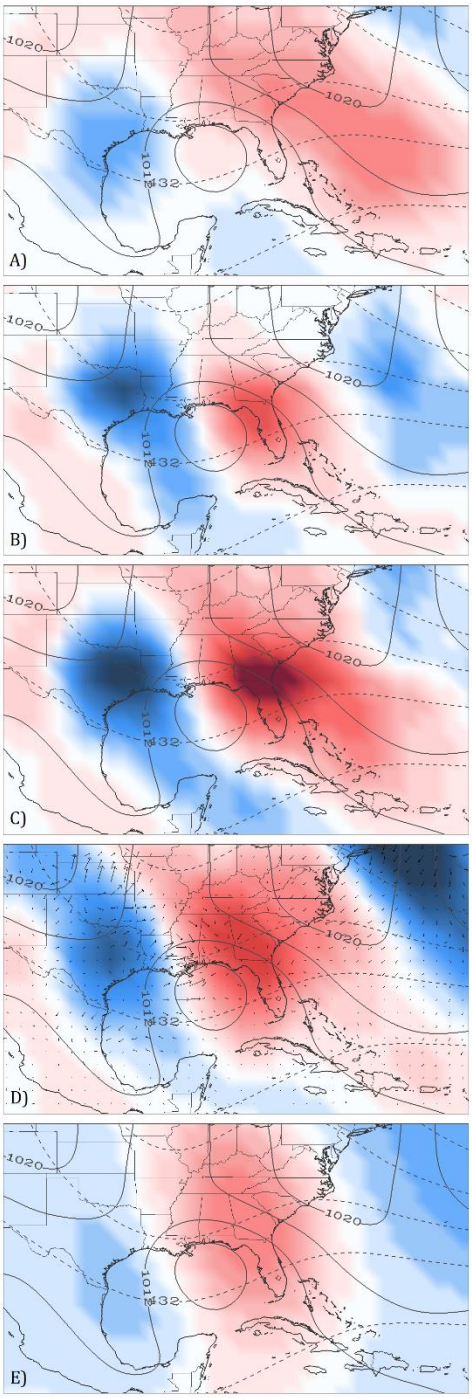

Fig. 1: 12:00 UTC 19 December 2009. **A)** Differential absolute vorticity advection by the geostrophic wind; **B)** minus the Laplacian of the temperature advection by the geostrophic wind; **C)** RHS of the adiabatic traditional form of the quasi-geostrophic omega equation; **D)** RHS of the adiabatic $\vec{Q}$-vector formulation of the quasi-geostrophic omega equation and vector field of the $\vec{Q}$-vector; **E)** analyzed omega. Each map includes the sea-level pressure field (solid line) and the geopotential height field at the 600-hPa level (dashed line). Note that red-shaded (blue-shaded) areas are related to upward (downward) vertical motion.

A. Storm Aurore, 21/10/21 (18:00 UTC) B. Storm Eunice, 18/02/22 (06:00 UTC) C. 08/03/22 (18:00 UTC)

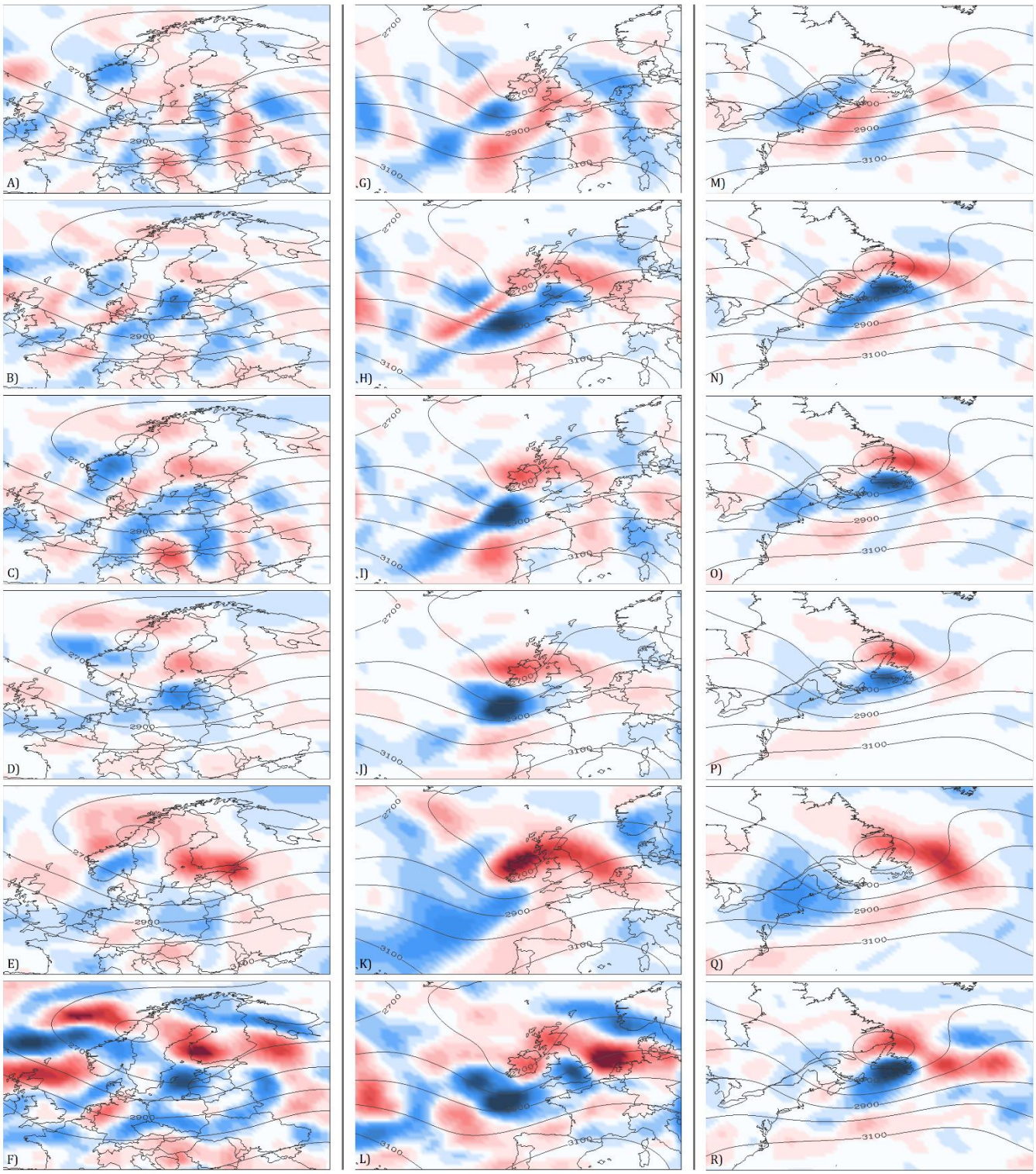

Fig. 2: Each column represents one of the analyzed case studies and displays: **A)**, **G)**, **M)** differential absolute vorticity advection by the geostrophic wind; **B)**, **H)**, **N)** minus the Laplacian of the temperature advection by the geostrophic wind; **C)**, **I)**, **O)** RHS of the adiabatic traditional form of the quasi-geostrophic omega equation; **D)**, **J)**, **P)** RHS of the adiabatic $\vec{Q}$-vector formulation of the quasi-geostrophic omega equation; **E)**, **K)**, **Q)** analyzed omega; and **F)**, **L)**, **R)** RHS of the diabatic $\vec{Q}$-vector formulation of the quasi-geostrophic omega equation. All fields are calculated at the 700-hPa level and include the geopotential height field at this level. Note that red-shaded (blue-shaded) areas are related to upward (downward) vertical motion.

As for the $\vec{Q}$-vector (Fig. 2J), the areas of convergence (divergence) match the regions of upward (downward) vertical motion inferred from the traditional form of the Q-G omega equation (Fig. 2I) along the axis of the trough, and they also agree with the actual vertical motion in that region, given by the analyzed omega chart. Note that, for this case, these fields are less noisy than for the previous one, and, although they indicate more localized areas for ascent and descent than actually observed, both the $\vec{Q}$-vector and the traditional forms of the Q-G omega equation provide a better match to the real omega than in the previous case.

C. 08/03/22 (18:00 UTC) – 700 hPa

Focusing on the analyzed omega plot (Fig. 2Q), one can identify an extensive area of upward vertical motion in the western North Atlantic accompanied by a region of downward vertical motion to the west of the trough axis. No clear conclusion can be drawn from the comparison of the DVA and LTA terms (Fig. 2M and Fig. 2N, respectively) since, again, there is a large amount of cancellation between them. Here, the LTA term is also the dominant one (Fig. 2O), and it is also similar to the actual pattern of analyzed vertical motion given by the analyzed omega field.
For this case, the traditional form of the Q-G omega equation (Fig. 2O) and the divergence of the $\vec{Q}$-vector (Fig. 2P) provide almost identical patterns for vertical motion, which in turn agree with the analyzed one. This is the case for which the best match between the Q-G diagnosis and reality is obtained.

V. THE RELEVANCE OF THE NEGLECTED CONTRIBUTIONS

The former discussion on the Q-G theory applicability for real case studies is based on the adiabatic forms of the traditional and $\vec{Q}$-vector formulations of the Q-G omega equation, but these equations can be rendered more complete by taking into account the contribution of diabatic heating (especially the latent heat release). This term cannot be computed explicitly, but for our purposes it may be obtained as a residual from the thermodynamic equation. Its contribution to Eq. (1) and (2) can be written as

$$-\frac{\kappa}{p}\nabla^2 J = -\frac{R}{p}\nabla^2\left(\frac{\partial T}{\partial t}+\frac{T}{\theta}\frac{\partial \theta}{\partial p}\omega+\vec{V}\cdot\nabla T\right), \qquad (4)$$

where $\kappa = R/c_p$, c_p is the specific heat capacity at constant pressure, J the rate of heating, and $\vec{V}$ the full wind vector. This residual has been added to the adiabatic expressions, Eq. (1) and (2) and is shown in the bottom row of Fig. 2 for each case. Even though diabatic heating appears to be less important in case C, in that it does not substantially change the pattern of vertical motion, we see that it cannot be neglected in cases A and B, since it provides an important contribution to the pattern. Note, however, that even accounting for latent heating, there are still discrepancies between the spatial distribution of vertical motion arising from the Q-G analysis and the actual one. These may be attributed to all the ageostrophic terms and the orographic forcing (upslope and downslope flow) that have been assumed to be negligible.

VI. CONCLUSIONS

- The assessment of vertical motion by separately analyzing the DVA and LTA terms of the traditional Q-G omega equation is problematic due to the cancellation problem. Additionally, there is not clear rule to establish which term is the most relevant as either can dominate depending on the particular case (not shown).
- In general, the two appraised Q-G diagnostic methods (Eq. (1) and (2)) provide more accurate patterns for vertical motion along the axis of the trough.
- Even though Eq. (1) involves vertical derivatives, which imply an additional approximation in the calculation, both formulations of the Q-G omega equation yield similar quality diagnostics.
- Q-G analysis for diagnosing vertical motion provides accurate results when the Q-G assumptions are fulfilled, as shown for the textbook case. However, when examining real case studies, the diagnosed pattern for vertical motion matches the actual one only in certain regions within the low-pressure disturbances. The contribution of the neglected terms such as diabatic heating, the ageostrophic terms, or the orographic forcing accounts for the discrepancies between the Q-G-estimated and the actual vertical motion.

Acknowledgments

I would like to thank my advisor, Dr. Ileana Bladé, for her guidance throughout this project and for patiently providing helpful suggestions and corrections whenever needed. I would also like to thank my family and closest friends for their support during these months.

[1] J. E. Martin, Mid-Latitude Atmospheric Dynamics: A First Course, John Wiley & Sons Ltd, 2006.

[2] K. Trenberth, "On the interpretation of the diagnostic quasi-geostrophic omega equation," *Monthly Weather Revire*, vol. 106, pp. 131-137, 1978.

[3] J. Martin, "On the Deformation Term in the Quasigeostrophic Omega Equation," *Monthly Weather Review*, vol. 126, pp. 2000-2007, 1998.

[4] B. J. Hoskins, I. Draghici and H. C. Davies, "A new look at the omega-equation," *Quart. J. R. Met. Soc.*, vol. 104, pp. 31-38, 1978.

[5] J. R. Holton, An Introduction to Dynamic Meteorology, Elsevier Academic Press, 2004.

[6] "Unidata," UCAR Community Programs, 2022. [Online]. Available: https://www.unidata.ucar.edu/software/idv/. [Accessed February 2022].

[7] "GMAO, MERRA 2," NASA, 2019. [Online]. Available: https://gmao.gsfc.nasa.gov/reanalysis/MERRA-2/. [Accessed April 2022].

[8] G. Lackmann, B. E. Mapes and K. R. Tyle, Synoptic-Dynamic Meteorology Lab Manual, American Meteorological Society, 2017.